Synthetic and Systems Biotechnology 9 (2024) 381–390

Contents lists available at ScienceDirect

Synthetic and Systems Biotechnology

journal homepage: www.keaipublishing.com/en/journals/synthetic-and-systems-biotechnology

Original Research Article

Genus-specific secondary metabolome in *Allokutzneria* and *Kibdelosporangium*

Man-Jing Ma [a,1], Wen-Chao Yu [a,1], Huai-Ying Sun [a], Bing-Cheng Dong [a], Gang-Ao Hu [a], Zhen-Yi Zhou [a], Yi Hua [a], Buddha Bahadur Basnet [a,b], Yan-Lei Yu [a], Hong Wang [a,**], Bin Wei [a,*]

[a] College of Pharmaceutical Science & Collaborative Innovation Center of Yangtze River Delta Region Green Pharmaceuticals, Zhejiang Key Laboratory of Green, Low-Carbon, and Efficient Development of Marine Fishery Resources, Zhejiang University of Technology, Hangzhou 310014, China
[b] Central Department of Biotechnology, Tribhuvan University, Kathmandu, Nepal

ARTICLE INFO

Keywords:
Genus-specific secondary metabolism
Allokutzneria
Kibdelosporangium
Genome mining
Untargeted metabolomics
Siderophore

ABSTRACT

Rare actinomycete genera are highly recognized as a promising source of structurally diverse and bioactive natural products. Among these genera, *Allokutzneria* and *Kibdelosporangium* are two phylogenetically closely related and have been reported to encode some valuable biosynthetic enzymes and secondary metabolites. However, there is currently no relevant systematic research available to outline the linkage of genomic and metabolomics for specific secondary metabolites in these two promising genera. In this study, we first investigated the genus-specific secondary metabolic potential in *Allokutzneria* and *Kibdelosporangium* by comparing the diversity and novelty of their secondary metabolite biosynthetic gene clusters (BGCs). The specific secondary metabolites produced by two representative strains of these genera were comprehensively investigated using untargeted metabolomics techniques. The findings unveiled that the majority (95.4%) of the gene cluster families (GCFs) encoded by *Allokutzneria* and *Kibdelosporangium* were genus-specific, including NRPS GCFs encoding siderophores. The untargeted metabolomics analysis revealed that the metabolic profiles of two representative strains exhibit extensive specificity, with the culture medium having a big impact on the metabolic profiles. Besides, an MS-cluster featuring a series of hydroxamate-type siderophores was identified from *Allokutzneria albata* JCM 9917, with two of them, including a novel one (N-deoxy arthrobactin A), being experimentally validated. The present study offers valuable insights for the targeted discovery of genus-specific natural products from microorganisms.

1. Introduction

Over the past few decades, actinobacteria have consistently been one of the major sources of microbial secondary metabolites [1]. Among them, *Streptomyces* is the most prominent genus in Actinobacteria, known for its remarkable ability to produce valuable secondary metabolites such as antibiotics, anticancer drugs, immunosuppressants, and enzyme inhibitors [2]. Unfortunately, due to the growing number of active compounds isolated from *Streptomyces*, it has become increasingly challenging to discover novel natural products from this genus. Currently, a rapid surge of new compounds with broad biological activity and pharmacological properties are being discovered from non-*streptomyces* actinobacteria, that is, rare actinobacteria [3]. Rare actinobacteria encompass over 200 genera, including *Actinomadura*, *Allokutzneria*, *Amycolatopsis*, *Catenuloplanes*, *Cystobacter*, *Kibdelosporangium*, *Kutzneria*, *Pseudonocardia*, *Saccharomonospora*, *Thermomonospora*, *Virgosporangium* and so on [4].

The genus *Kibdelosporangium* was first proposed by Shearer et al., in 1986 [5] and comprised ten recognized species and subspecies. *Kibdelosporangium* strains are renowned for their production of novel glycopeptide antibiotics, such as aridicins and kibdelins [6,7]. Based on the phylogenetic and chemotaxonomic characteristics, *K. albatum* has been reclassified as the "type species" of the new genus *Allokutzneria* by *Labeda and Kroppenstedt* in 2008 [8]. The genus of *Allokutzneria*

Peer review under responsibility of KeAi Communications Co., Ltd.
* Corresponding author.
** Corresponding author.
E-mail addresses: hongw@zjut.edu.cn (H. Wang), binwei@zjut.edu.cn (B. Wei).
[1] Man-Jing Ma and Wen-Chao Yu contributed equally to this article.

https://doi.org/10.1016/j.synbio.2024.03.015
Received 5 November 2023; Received in revised form 4 March 2024; Accepted 20 March 2024
Available online 21 March 2024

comprised three species, namely *A. albata*, *A. multivorans*, and *A. oryzae* [9]. Although the number of species within these two genera is relatively small, many intriguing natural products and biosynthetic enzymes have been characterized from these strains. For instance, two novel N-phenylacetylated heptapeptides have been isolated from *Kibdelosporangium* sp. AK-AA56 [10]. Similarly, two diterpene synthases and their catalytic products spiroalbatene and cembrene A have been identified from *A. albata* [11].

Genome mining studies have suggested the presence of a substantial number of secondary metabolite biosynthetic gene clusters (BGCs) in these rare actinomycetes [12]. Our recent findings have uncovered that *Kibdelosporangium* possesses the highest secondary metabolic potential among bacterial genera, with an average of 40 BGCs per genome [13]. *Allokutzneria* is phylogenetic closely related to *Kutzneria* and *Kibdelosporangium*, our recent study has demonstrated that *Kutzneria* exhibited great potential to synthesize novel secondary metabolites and encode a variety of valuable biosynthetic enzymes [14]. These findings lead us to contemplate whether the secondary metabolic potential of these phylogenetic closely related genera is comparable to each other and explore the specific secondary metabolites from these strains.

In this study, we first compared the specific secondary biosynthetic potential of *Allokutzneria* and *Kibdelosporangium* by examining the distribution of BGCs in these two genera. Then, the secondary metabolites produced by two representative strains of these genera were investigated under different culture conditions using untargeted metabolomics. Furthermore, an MS-cluster featuring a series of specific secondary metabolites was preliminarily identified using UPLC-QTOF/MS, and two of these metabolites were extensively characterized by HR-MS/MS, 1D, and 2D NMR, and their biological activity was determined.

2. Materials and methods

2.1. Genome dataset and bacterial strains

All available genome sequences from *Allokutzneria* and *Kibdelosporangium* were manually downloaded from the NCBI database. The GenBank accession number, genome size, and taxonomic information of all the genomes were collected and summarized in Supplementary Table 1. Genome assembly quality was assessed by CheckM version 1.2.2 [15]. *Allokutzneria albata* JCM 9917 and *Kibdelosporangium phytohabitans* KLBMP1111 were obtained from the German Collection of Microorganisms and Cell Cultures GmbH (DSMZ) and Ningbo testobio. Co., Ltd, Zhejiang, China, respectively.

2.2. Biosynthetic gene cluster identification and networking

All genome sequences were processed using the online version of antiSMASH 7.0 with the bacterial setting and relaxed strictness [16]. The number of each class of BGCs in these genomes was extracted from the HTML files (antiSMASH outputs) using a custom Python toolkit, as described in our previous report [17]. The genomic features and numbers of BGCs in each genome were also summarized inSupplementary Table 1. All predicted BGCs were assigned to different biosynthetic gene cluster families (GCFs) using BiG-SLiCE at a distance cutoff of 0.5 [18]. The specificity of GCF depends on whether the BGCs in it originate from a single bacterial genus or not. The origin, class, GCF classification result, and specificity of each BGC were summarized in Supplementary Table 2.

2.3. High-Throughput elicitor screening (HiTES) for A. albata JCM 9917 and K. phytohabitans KLBMP1111

A. albata JCM 9917 and *K. phytohabitans* KLBMP1111 were cultured under nine different liquid media (M1: GYE; M2: DSMZ 554; M3: JCMM 58; M4: JCMM 44; M5: JCMM 42; M6: GYM; M7: R5M; M8: TSB; M9: NL148) for three days, then six previously reported chemical elicitors, namely $LaCl_3{\cdot}7H_2O$ [31], $ScCl_3{\cdot}6H_2O$ [32], N-acetylglucosamine (NAG) [33], sodium butyrate [34], streptomycin in combination with trimethoprim (TMP) [35], and triclosan [36], were individually supplemented to the cultures and allowed to incubate for an additional seven days. Simultaneously, the blank and control groups were set for subsequent analysis. All HiTES screens were carried out in a single replicate. The culture broth was extracted by an equal volume of ethyl acetate and analyzed using a UPLC-QTOF/MS system (SCIEX X500B Q-TOF spectrometer coupled to an ExionLC AC system) according to our recent report [17].

2.4. Molecular networking and annotation of MS/MS data

The high-resolution liquid chromatography-mass spectrometry (LC-HRMS) data was converted using MSConvert, and processed using MZmine2 software [19]. Feature detection, grouping, alignment, and molecular networking were performed following the feature-based molecular networking (FBMN) and the Dereplicator + workflow in GNPS (http://gnps.ucsd.edu) [20,21]. Molecular networks were generated with a minimum of four matching peaks, a cosine score of 0.7, and a maximum of 250 connected component sizes. The SIRIUS 4 was also employed for feature annotation with the default settings [22]. The molecular network generated from FBMN was visualized by using Cytoscape 3.6.1. The mirror match of spectra was constructed using a Python package spectrum_utils using a custom Python toolkit [23]. All MS/MS peaks are listed in Supplementary Table 3.

2.5. Fermentation, isolation, and structure elucidation

JCM medium 42 and elicitor E (streptomycin in combination with TMP) were selected for large-scale fermentation of *A. albata* JCM 9917. For 15 L fermentation, seed inoculum was cultured in 500 mL Erlenmeyer flasks containing 200 mL medium at 30 °C for 72 h on a shaker incubator at 180 r.p.m. Aliquot (5–6 mL) of the seed culture was inoculated into each of 2000 mL Erlenmeyer flasks containing 1000 mL of the JCM medium 42. The microorganism was cultured at 30 °C for 14 days in a shaker incubator at 180 r.p.m. Then, the 15 L fermentation broth collected from cultures grown in 2 L Erlenmeyer flasks was centrifuged to remove cells, and the resulting supernatant was extracted with n-butanol and evaporated for concentration. The crude extract was eluted by MCI gel with gradient elution using $MeOH/H_2O$ (from 10:90 to 100:0). The targeted fraction was further purified by semi-prep-HPLC with gradient elution using $MeOH/H_2O$ (from 40:60 to 90:10 over 25 min) at a flow rate of 3 mL/min to yield two pure compounds **1** (20 mg) and **2** (5 mg).

2.6. Chrome azurol S (CAS) assay

The iron-chelating activity of compounds **1** and **2** was assessed using a modified CAS assay as described in our recent study [24]. The cetyltrimethylammonium bromide (CTAB)-CAS-Fe(III) solution was prepared by mixing 25 mL of CTAB solution (2 mM), 1.5 mL of $FeCl_3$ solution (1 mM), and 7.5 mL of CAS solution (2 mM). The CAS assay solution was obtained by adding the CAS-Fe(III) solution into the MES buffer. The test compounds were mixed with CAS solution and then incubated at 30 °C for 3 h, the resulting color changes were recorded by measuring the absorption changes at 630 nm. DFOB (Desferrioxamine B) is used as a positive control, and MeOH (methanol) is used as a negative control.

3. Results

3.1. Genomic features and the overall distribution of BGCs in Allokutzneria and Kibdelosporangium

To assess the secondary metabolite potential of *Allokutzneria* and

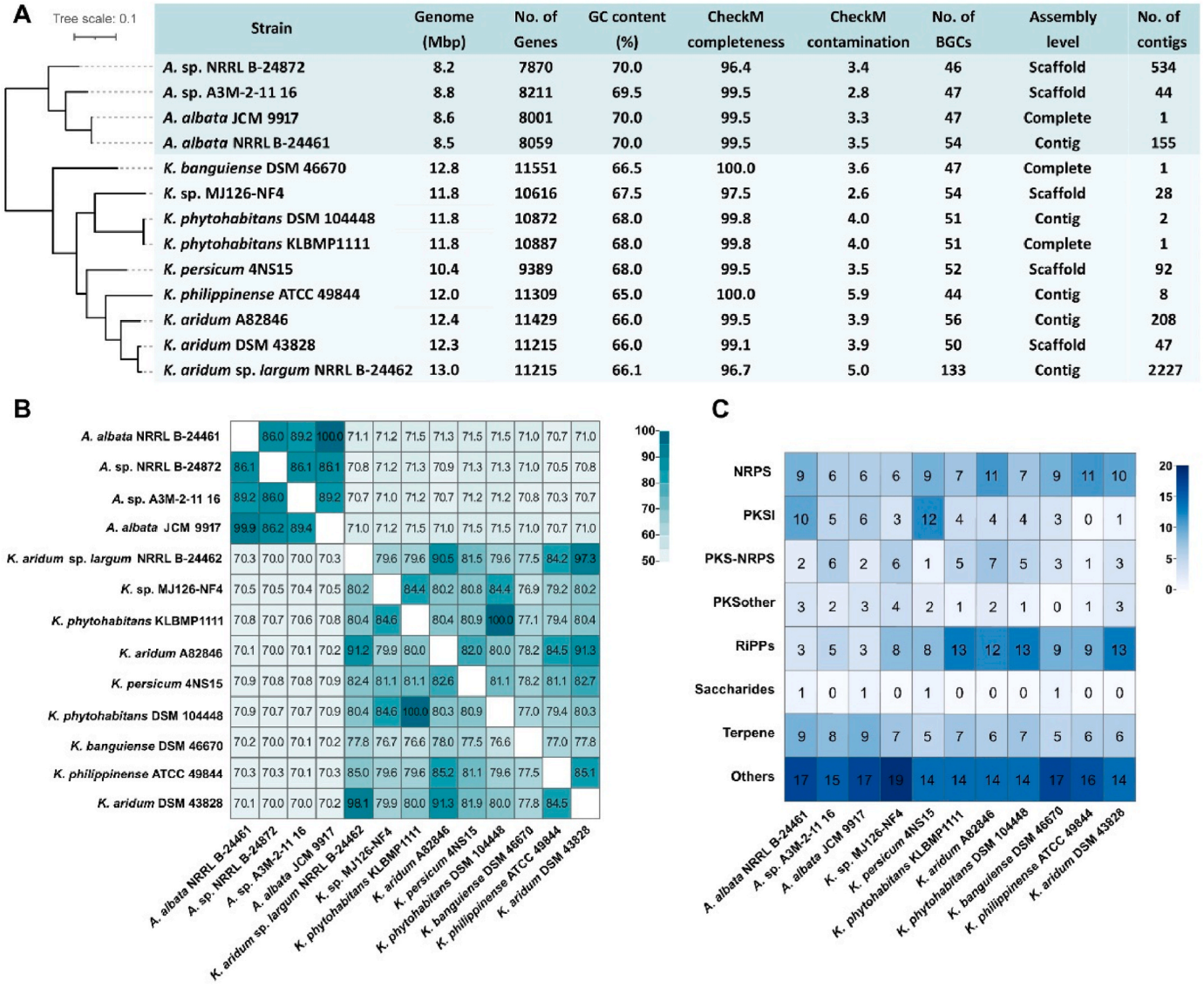

Strain	Genome (Mbp)	No. of Genes	GC content (%)	CheckM completeness	CheckM contamination	No. of BGCs	Assembly level	No. of contigs
A. sp. NRRL B-24872	8.2	7870	70.0	96.4	3.4	46	Scaffold	534
A. sp. A3M-2-11 16	8.8	8211	69.5	99.5	2.8	47	Scaffold	44
A. albata JCM 9917	8.6	8001	70.0	99.5	3.3	47	Complete	1
A. albata NRRL B-24461	8.5	8059	70.0	99.5	3.5	54	Contig	155
K. banguiense DSM 46670	12.8	11551	66.5	100.0	3.6	47	Complete	1
K. sp. MJ126-NF4	11.8	10616	67.5	97.5	2.6	54	Scaffold	28
K. phytohabitans DSM 104448	11.8	10872	68.0	99.8	4.0	51	Contig	2
K. phytohabitans KLBMP1111	11.8	10887	68.0	99.8	4.0	51	Complete	1
K. persicum 4NS15	10.4	9389	68.0	99.5	3.5	52	Scaffold	92
K. philippinense ATCC 49844	12.0	11309	65.0	100.0	5.9	44	Contig	8
K. aridum A82846	12.4	11429	66.0	99.5	3.9	56	Contig	208
K. aridum DSM 43828	12.3	11215	66.0	99.1	3.9	50	Scaffold	47
K. aridum sp. *largum* NRRL B-24462	13.0	11215	66.1	96.7	5.0	133	Contig	2227

Fig. 1. (**A**) Genomic features of four *Allokutzneria* genomes and nine *Kibdelosporangium* genomes. (**B**) Genomic similarities between thirteen genomes were measured by the pattern similarity score. (**C**) The numbers of each class of BGCs in the 11 high-quality genomes of *Allokutzneria* and *Kibdelosporangium*.

Kibdelosporangium, we collected all the available genome sequences for both genera and conducted an in-depth bioinformatic analysis. Our findings suggest that the strains of these two genera exhibited significant differences in genomic characteristics. In comparison to *Kibdelosporangium* genomes, the genomes of *Allokutzneria* exhibit slightly smaller sizes and lower number of genes, while their GC content is higher than that of *Kibdelosporangium* (Fig. 1A). It is worth noting that there exists a significant inter-generic difference in the similarity between these two genera. Genomes within the *Allokutzneria* genus share a sequence similarity above 86%, while in the *Kibdelosporangium* genus, the similarity is above 76% (Fig. 1B). The similarity between genomes from these two different genera ranges from 70% to 71.5% (Fig. 1B). These findings further confirm that *Allokutzneria* is a distinct genus separate from *Kibdelosporangium*. The total numbers of predicted BGCs in these genomes range from 46 to 56, except for *Kibdelosporangium aridum* subsp. *largum* NRRL B-24462, showed no significant difference between these two genera (Fig. 1A). The genome of *K. aridum* subsp. *largum* NRRL B-24462 showed a completeness of 96.7% and a contamination rate of up to 5%. It contained 2227 contigs, and the fragmented genome resulted in an overestimated number of BGCs (Fig. 1A). Therefore, we selected 11 high-quality genomes from the two genera and counted the number of each class of BGCs in these genomes (Table S1). The results show that NRPS, PKSI, and Terpene are the top three dominant classes of BGCs in the genomes of the *Allokutzneria*, while RiPPs, NRPS, and Terpene are the top three dominant in the *Kibdelosporangium* genomes (Fig. 1C). For instance, the number of RiPPs BGCs in *Kibdelosporangium* is approximately three times higher compared to *Allokutzneria*, with an average of 10.63 versus 3.67. Besides, both genera possess a wide variety of BGC types, and many of them are classified as "Others". Notably, the genomes of two strains of the same species (*Allokutzneria albata* NRRL B-24461 and *Allokutzneria albata* JCM 9917) have extremely high genomic similarity (Fig. 1B). Nevertheless, they showed some difference in the numbers of NRPS and PKSI BGCs (Fig. 1C), which was mainly due to some larger NRPS and PKSI BGCs being located at the edges of contigs, resulting in the overestimation.

3.2. Genus-specific secondary metabolic potential in Allokutzneria and Kibdelosporangium

The diversity and novelty of all 553 BGCs predicted from the 11 high-quality genomes were investigated using BiG-SCAPE. The results showed that these BGCs were divided into 304 gene cluster families

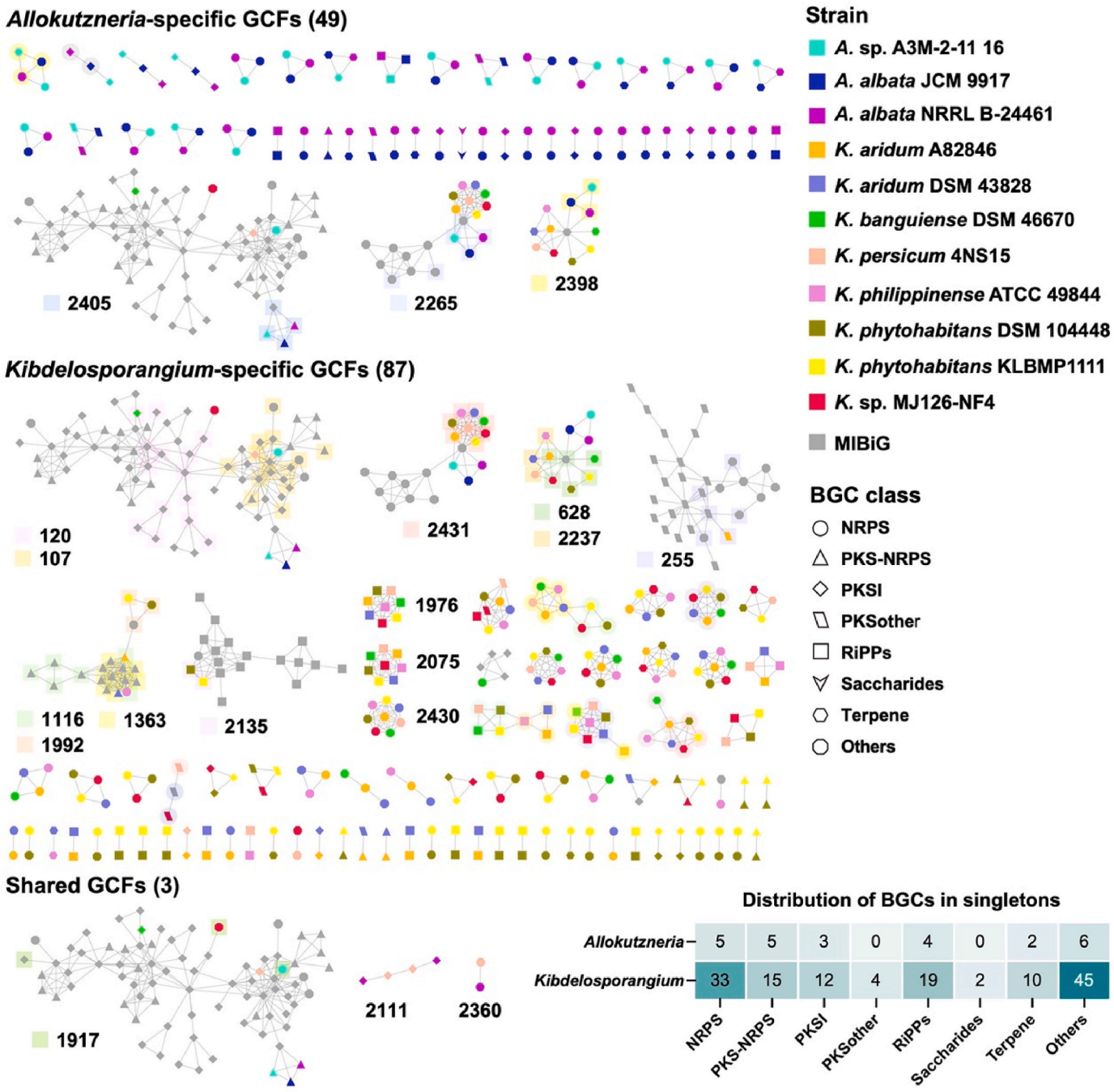

Fig. 2. Sequence similarity network of BGCs in 11 high-quality *Allokutzneria* and *Kibdelosporangium* genomes. Each node represents one BGC, and the gray symbols represent BGCs from the MIBiG database. BGCs distributed within the same cluster but belonging to different GCFs were differentiated using background colors. The heatmap displays the number of different classes of BGCs within the singletons of these two genera.

(GCFs) at a threshold of 0.5. Among them, 139 GCFs contained at least two BGCs, while the remaining 165 GCFs were singletons. Out of the 304 GCFs obtained, only 14 GCFs contained characterized BGCs from the MIBiG database, implying that a significant majority (95.4%) of these GCFs remain unexploited. Besides, 74 GCFs (including 49 GCFs containing more than two BGCs and 25 singletons) are specific to the *Allokutzneria*, 227 GCFs (including 87 GCF containing more than two BGCs and 140 singletons) are unique to the *Kibdelosporangium*, and only 3 GCFs are shared between them, demonstrating a remarkable specificity in the secondary metabolic potential between *Allokutzneria* and *Kibdelosporangium*. Three genomes of *Allokutzneria* encoded 52 GCFs with more than two BGCs and 25 singletons. *Allokutzneria albata* shared 23 GCFs with *Allokutzneria* sp. A3M-2–11, including two GCFs encoding elaiophylin (no. 2405) and ectoine (no. 2265) analogous, respectively. Notably, *A. albata* also contained 23 species-specific GCFs that were not present in *Allokutzneria* sp. A3M-2–11 16, and all of them did not contain known BGCs from the MIBiG database. Eight genomes of *Kibdelosporangium* encoded 90 GCFs with more than two BGCs and 140 singletons. Only four GCFs were found to contain BGCs from all eight strains of *Kibdelosporangium*, suggesting that the remaining GCFs exhibited a certain degree of species-specificity (Fig. 2). Majority of the BGCs in the singletons of *Kibdelosporangium* were originated from others, NRPS, and RiPPs, suggesting that different species of *Kibdelosporangium* have the potential to produce species-specific and biosynthetically complex

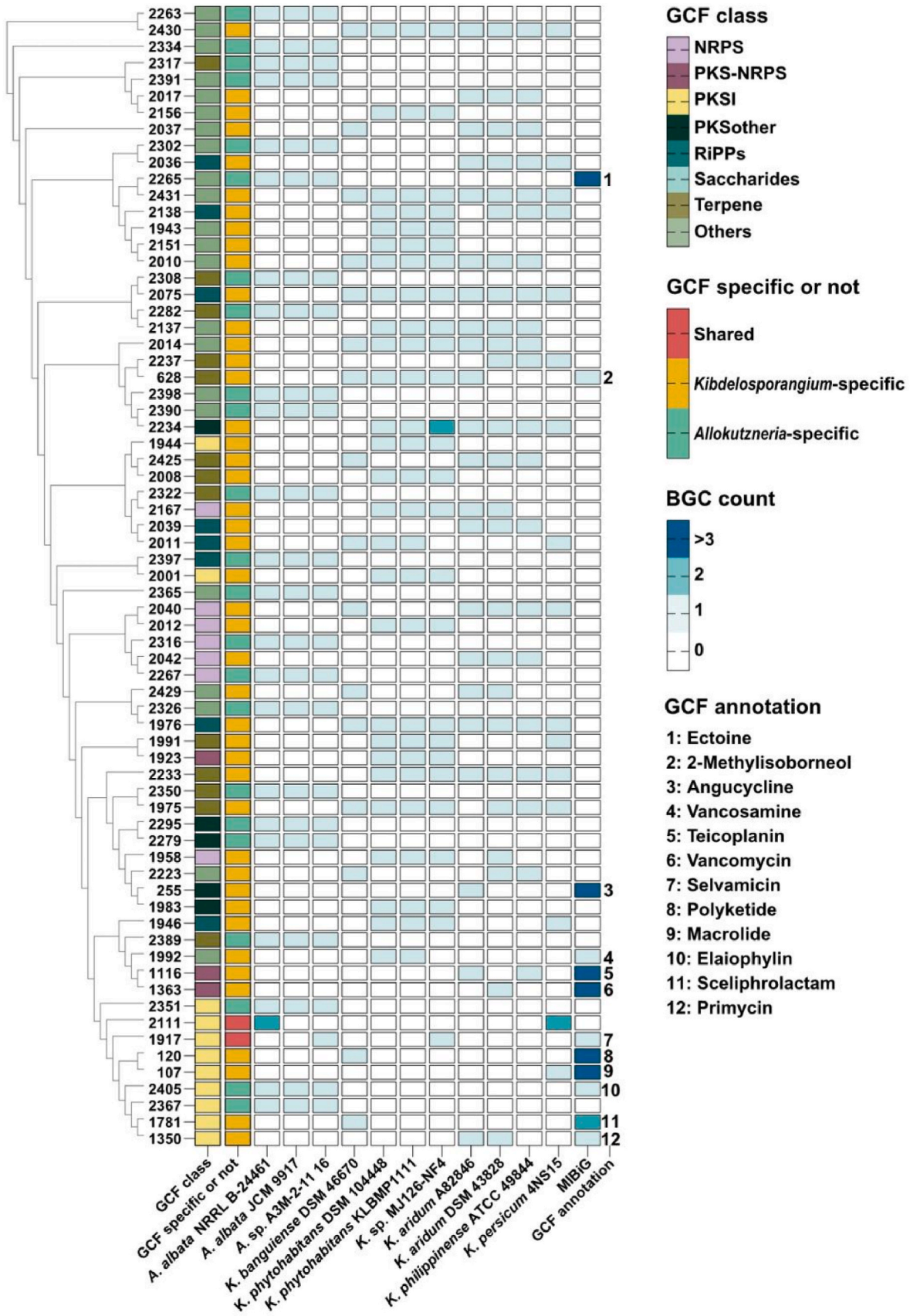

Fig. 3. The hierarchical clustering dendrogram of 69 GCFs containing more than three BGCs and the distribution of these BGCs within *Allokutzneria* and *Kibdelosporangium*. The GCF class and its specificity were presented in the heatmap. GCFs were annotated based on the characterized metabolites encoded by BGCs from the MIBiG database.

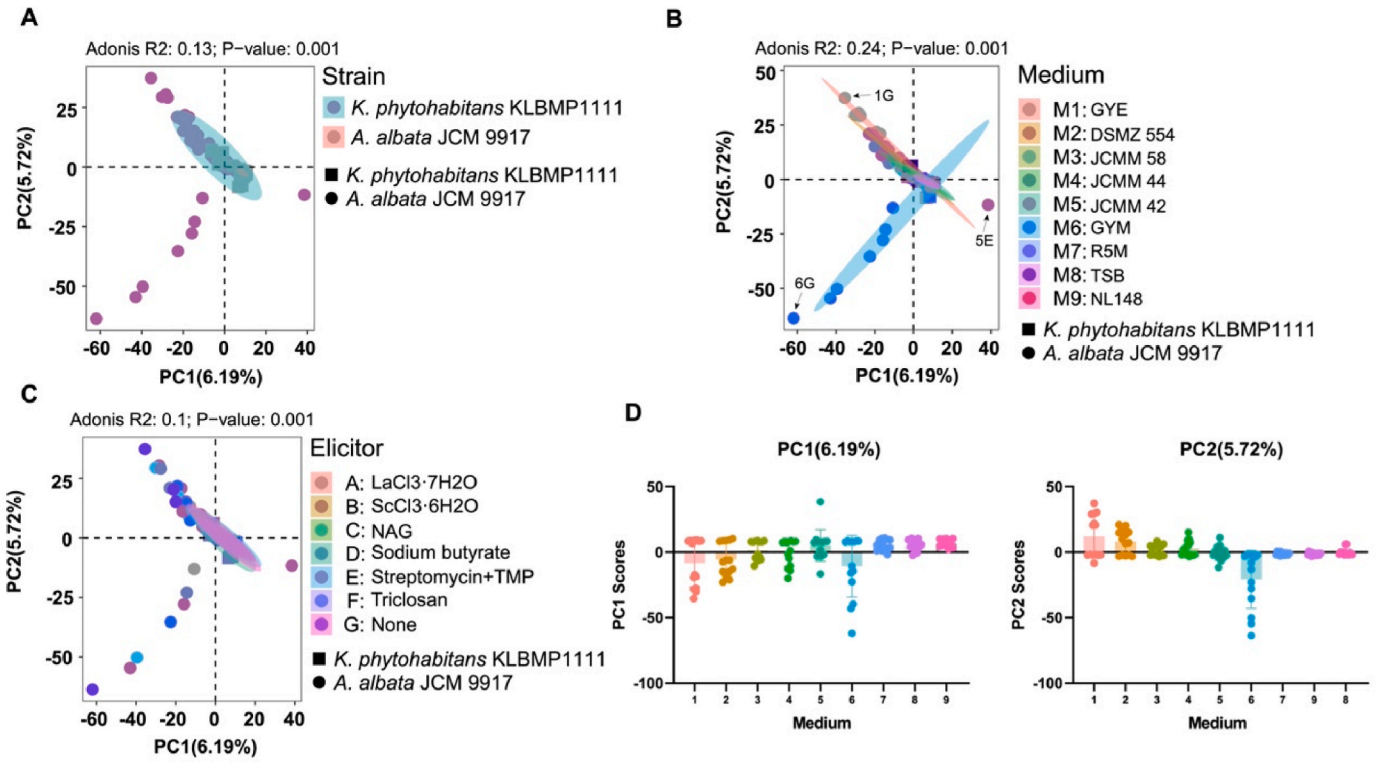

Fig. 4. Principal Component Analysis (PCA) of the metabolic profiles of *A. albata* JCM 9917 and *K. phytohabitans* KLBMP1111 under nine different culture media and six elicitors. Samples were colored according to the type of (**A**) strain, (**B**) culture media, and (**C**) elicitor. (**D**) The principal component values of samples when divided according to the culture media.

natural products, particularly peptidic natural products.

The distribution of BGCs in 69 predominant GCFs was presented in Fig. 3, further confirming the genus-specificity of *Allokutzneria* and *Kibdelosporangium* in secondary metabolic potential. Among these GCFs, 12 of them tentatively annotated according to the characterized metabolites encoded by BGCs from the MIBiG database, which mainly belonged to three major classes: PKSI [6], PKS-NRPS hybrid [2], and others [2]. For instance, *Allokutzneria* sp. A3M-2–11 16 and *Kibdelosporangium* sp. MJ126-NF4 were predicted to be capable of synthesizing selvamicin analogous (PKSI products). *Kibdelosporangium aridum* A82846, *Kibdelosporangium aridum* DSM 4328, and *Kibdelosporangium philippinense* ATCC 49844 encoded a PKS-NRPS BGC for the synthesis of glycopeptide antibiotics, but these three BGCs were divided into two GCFs (nos. 1116 and 1363), which are highly homologous to the BGCs encoding vancomycin and teicoplanin, respectively. Notably, all seven NRPS and eight RiPPs GCFs were genus-specific and showed high potential to produce novel peptidic natural products. The hierarchical clustering dendrogram of these GCFs was established using clinker, based on the sequence similarity matrix of similar genes in representative BGCs. Consequently, the GCFs that share biosynthetic similarities were gathered together. For instance, parts of the BGCs within two genetically closely related GCFs (nos. 2265 and 2431) were connected to each other in the network indicating a certain degree of similarity as well as noticeable differences between these BGCs. Comparative analysis of these BGCs revealed that they all contain ectoine synthase, parts of them harbored genes encoding aldo/keto reductases, and only BGCs in GCF 2431 contained genes encoding GDSL-like lipase/cylhydrolase and cyclic nucleotide-binding domain (Supplementary Fig. 1). Each of the three strains of *Kibdelosporangium* encoded a homologous gene cluster for either vancomycin or teicoplanin, which are distributed in two different GCFs (nos. 1116 and 1363). There are significant differences in the predicted substrates of the adenylation domains of their NRPS enzymes (Supplementary Fig. 2).

3.3. Specific secondary metabolites in Allokutzneria and Kibdelosporangium

To investigate the specific secondary metabolites in *Allokutzneria* and *Kibdelosporangium*, *A. albata* JCM 9917 and *K. phytohabitans* KLBMP1111, which possess complete genomes and display a remarkable diversity and novelty of BGCs, were selected as the representative species for each genus. The secondary metabolites of these two strains were extensively studied using the HiTES approach. The HiTES experiment mainly investigated the impact of nine different culture media and six chemical elicitors on the specific secondary metabolites of these two strains by comparing the metabolic profiles with control samples that were prepared without elicitors or strains. The ethyl acetate extracts of these samples were analyzed using an untargeted metabolomics approach with LC-HRMS. The relative abundance of the detected metabolite features in these samples was subjected to principal component analysis (PCA). As shown in Fig. 4A–C, the secondary metabolites produced by *A. albata* JCM 9917 and *K. phytohabitans* KLBMP1111 exhibited significant differences from each other (Adonis $R^2 = 0.13$, $p < 0.001$), and the metabolic profiles are also significantly affected by both culture media (Adonis $R^2 = 0.24$, $p < 0.001$) and chemical elicitors (Adonis $R^2 = 0.1$, $p < 0.001$). The principal component values indicated that culture media 6 (GYM), 5 (JCMM 42), and 1 (GYE) have a significant impact on the metabolic profiles of some samples of the two strains (Fig. 4D), particularly in the case of 6G (cultured in GYM without elicitor), 5E (cultured in JCMM 42 under the induction of streptomycin and trimethoprim), and 1G (cultured in GYE without elicitor).

We further analyze the diversity and novelty of secondary metabolites produced by these two strains in the HiTES experiment using GNPS and related annotation platforms (FBMN, Dereplicator+, and SIRIUS). Among the 991 features detected under the culture media of M5, M7, and M8, 510 of them were unique to *A. albata* JCM 9917, 210 were unique to *K. phytohabitans* KLBMP1111, and the rest were detected in

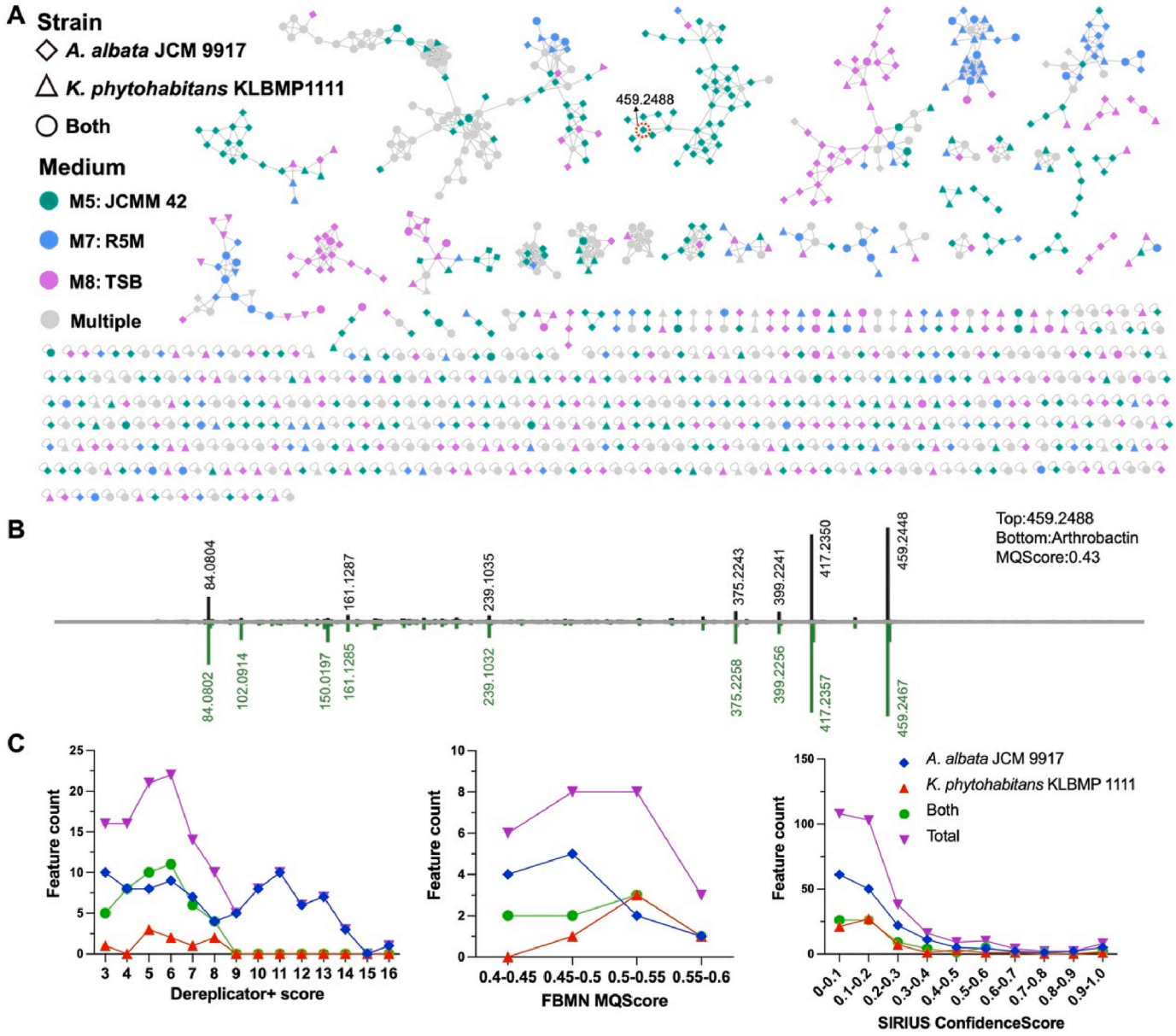

Fig. 5. (**A**) Molecular network of secondary metabolites produced by *A. albata* JCM 9917 and *K. phytohabitans* KLBMP1111 in the HiTES experiment. Features were colored according to the culture media and shaped according to the presence or absence of these two strains. Features were annotated by three methods (Dereplicator+, FBMN, and SIRIUS), and a unique compound is annotated in the figure. (B) The mirror MS/MS plot of the selected feature and Arthrobactin. (**C**) The number and composition of features annotated by Dereplicator+, FBMN, and SIRIUS at various thresholds.

both strains (Supplementary Table 4), highlighting the former strain possessed a higher chemical diversity. These features were categorized into 69 molecular families (MFs) and 475 singletons at a cosine similarity cut-off of 0.6. It can be observed that features in some MFs are exclusively derived from a single culture medium, particularly the M5 (JCMM 42) and M8 (TSB) media (Fig. 5A). For example, nearly all features in the MF containing a feature annotated as arthrobactin (FBMN MQscore = 0.43) were only detected in samples cultured in JCMM 42. The Dereplicator + analysis identified 139 features with scores larger than 3. However, only 86 features had scores larger than 6 and p-values smaller than 0.001. The FBMN analysis yielded 25 features with MQScore greater than 0.4, with the majority (14/25) scoring between 0.4 and 0.5. The SIRIUS analysis yielded 26 features with Confidence Score greater than 0.5, and 51 features with Confidence Score greater than 0.3 (Fig. 5B). These findings indicated that the majority of these features were potential undescribed metabolites. Besides, these annotated features, under most annotation thresholds, mainly originated from samples of *A. albata* JCM 9917.

3.4. Characterization of specific secondary metabolites in Allokutzneria

Among the specific secondary metabolites produced by *A. albata* JCM 9917, two of them (**1** and **2**) showed high abundance and were assigned as arthrobactin analogs (Fig. 6A). Consequently, they were purified and structurally elucidated. The structures of Arthrobactin A (**1**) and N-deoxy arthrobactin A (**2**) were characterized by extensive analysis of 1D and 2D NMR spectroscopic data.

Arthrobactin A (**1**) was obtained as a yellow oil. The molecular formulas of compound 1 was established as $C_{20}H_{34}N_4O_8$ (*m/z* 459.2444 $[M+H]^+$, calcd 476.2449; *m/z* 481.2283 $[M+Na]^+$, calcd 481.2269) indicating six degree of unsaturation. The ^1H, and ^{13}C NMR (Table S5) of **1** revealed the presence of two methyl, twelve methylene, five

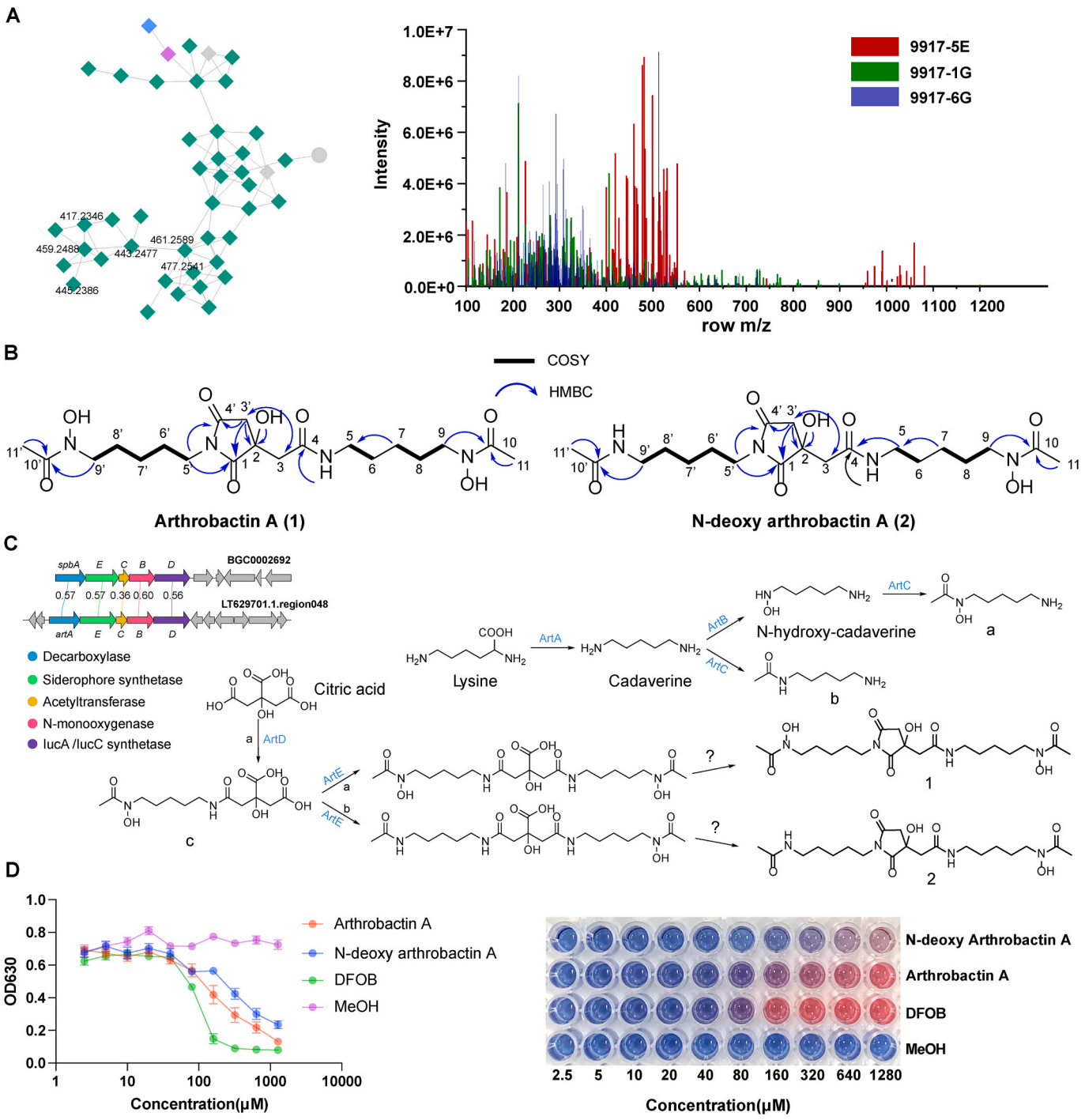

Fig. 6. (**A**) A group of specific secondary metabolites produced by *A. albata* JCM 9917. (**B**) Chemical structures of Arthrobactin A (**1**) and N-deoxy arthrobactin A (**2**), key COSY (bold lines), and HMBC (single-headed arrows) correlations for them. (**C**) Comparison of the *spb* and *art* gene clusters. The putative biosynthetic pathways for compounds **1** and **2**. (**D**) Fe(III)-binding properties of compounds **1** and **2** were assessed using CAS assay. The OD_{630} values were obtained after mixing the compound with CAS solution at different concentrations. DFOB (Desferrioxamine B) was used as a positive control, while MeOH served as a negative control.

carbonyls, and an oxygenated quaternary carbon. Comparison of ^{1}H and ^{13}C NMR data with HSQC correlations revealed that **1** has two amide carbonyl groups (δ_C 175.0 and 178.7). The ^{1}H–^{1}H COSY correlations of C5′ alkyl amine δ_H 3.32 (5′-H)/δ_H 1.48 (6′-H)/δ_H 1.20 (7′-H)/δ_H 1.48 (8′-H)/δ_H 3.44 (9′-H) and C5 alkyl amine δ_H 2.95 (5-H)/δ_H 1.35 (6-H)/δ_H 1.20 (7-H)/δ_H 1.48 (8-H)/δ_H 3.44 (9-H) allowed us to assemble two $(CH_2)_5$ moieties (Fig. 6B & Table S5). The long-range couplings observed in the HMBC experiments can be summarized (Fig. 6B) as follows: the cross-peaks from δ_H 3.32 (5′-H) to δ_C 178.7 (C-1) and δ_C 175.0 (C-4′), supported the presence of five-membered cyclic imide formed by condensation of citrate carboxyl with an amide of arthrobactin [25]. The cross-peaks from δ_H 1.96 (11-H/11′-H) to δ_C 170.2 (C-10/C-10′) supported the presence of two acetyl groups. The nitrogen-bearing methylene at δ_H 3.44 (9-H) showed a correlation with the carbonyl carbon at δ_C 170.2 (C-10), the same situation occurs in δ_H 3.44 (9′-H) and δ_C 170.2 (C-10′), thus establishing the connectivity of the C5 alkyl diamine to the N-acetyl group. Additionally, the correlation between δ_H 2.48 and 2.90 (3′-H), δ_H 2.61 and 2.75 (3-H), and δ_C 72.1 (C-2), led us to infer that the oxygenated carbon is linked to the two amide groups. Based on the molecular formula of **1**, it is estimated that the remaining atoms are

hydroxyl groups, one of which is attached to C-2, and the other two form N-hydroxyl groups.

The molecular formula of N-deoxy arthrobactin A (**2**) was established as $C_{20}H_{36}N_4O_7$ (*m/z* 443.2504 $[M+H]^+$, calcd 443.2500; *m/z* 465.2330 $[M+Na]^+$, calcd 465.2320). The ^{13}C NMR and HSQC spectra confirmed the presence of 20 carbons in **2**. Its NMR data were similar to those of **1** except, the protons on C-11' (δ_H 1.92) were more shielded than those on the other side at C-11 (δ_H 2.09) (Table S5), suggesting a proton was substituted by a hydroxyl group on one hydroxamate of **2**. Carefully examination of ^{13}C and 2D NMR of **2** concluded the structure of N-deoxy of **1**. We named this novel compound N-deoxy arthrobactin A.

The biosynthetic pathway for compounds **1** and **2** was proposed according to a recent report [26]. The *art* gene cluster showed a high sequence similarity to the previously putative *spb* gene cluster and contained all the essential genes encoding decarboxylase, acetyltransferase, L-lysine 6-monooxygenase, and siderophore synthetase (Fig. 6C). Meanwhile, the formation of a succinimide ring via the attack of the peptide bond nitrogen on the γ-carboxyl carbonyl represents a non-enzymatic reaction [30]. The sequence variations between the decarboxylase-encoding genes in these BGCs may be related to the length of the carbon chain in the final natural products. The Fe (III)-binding ability of Arthrobactin A and N-deoxy arthrobactin A was evaluated through CAS assay, and both compounds exhibited remarkable affinity for Fe(III). However, the former demonstrated superior binding activity compared to the latter. Both compounds bound to Fe (III) in a concentration-dependent manner, but their binding capacity was weaker compared to the positive control, DFOB, at multiple concentrations (Fig. 6D).

4. Discussion

Rare actinomycetes are one of the most promising sources of natural products. The in-depth genome mining of the rare actinomycetes plays a crucial role in the efficient discovery of natural products. The present study compared the secondary biosynthetic potential and metabolic profiles of *Allokutzneria* and *Kibdelosporangium* through comparative genomics and metabolomics approaches. Our findings demonstrated that these two genera showed great specificity in the distribution of the GCFs. The untargeted metabolomics study revealed that a type strain, *A. albata* JCM 9917, produced multiple series of specific natural products, including a series of hydroxamate-type siderophores.

Allokutzneria and *Kibdelosporangium* are two phylogenetically related genera and share 89.0%–95.4% sequence identity in 16S rRNA gene sequences [8]. To date, only fifteen natural products have been reported from these two genera [27], which is highly incompatible with the reported number of BGCs in these genera. In particular, to explore secondary metabolites from strains of these two genera, it is crucial to conduct a comprehensive comparison of their specificity in secondary metabolic potential. It is worth noting that the genomic data of these two genera are still insufficient, and the genome quality of some strains is poor. These limitations will have a certain impact on the assignment of genus-specific GCFs. However, most of the identified *Allokutzneria*-specific GCFs are highly conserved within the genus, indicating that the current data is sufficient to demonstrate the significant genus-specificity in secondary biosynthetic potential between these two genera. On the other hand, because of the challenges in acquiring strains, we only conducted an in-depth analysis on the secondary metabolites of two strains. Further research can be considered on the secondary metabolites of strains that exhibit obvious species-specificity in the distribution of GCFs.

The distance cutoff value of 0.3 was used as the default parameter to define GCFs in BiG-SCAPE. In the present study, to eliminate the influence of the limited number of genome sequences and analyze the specificity of GCFs in these two genera more accurately, we chose a more relaxed threshold of 0.5 to define GCFs. Even at this threshold, we still observed a substantial number of genus-specific GCFs in both genera, and there were evident structural differences among BGCs within phylogenetically related GCFs. The targeted exploration of natural products encoded by BGCs within these genus-specific GCFs using strategies such as heterologous expression or synthetic-bioinformatics natural product (syn-BNP) holds tremendous potential [28,29]. In addition, the genus *Kibdelosporangium* harbors many species-specific BGCs, whose encoded natural products are also worthy of further exploration. It is important to note that although most of the genus-specific GCFs do not include known BGCs from the MIBiG database, they still share some degree of similarity, and the genus-specific BGCs may encode metabolites that are structurally similar to the known BGCs. For instance, two siderophore BGCs discovered in a specific GCF of *Allokutzneria* show a similarity score of 0.28 to the gene cluster BGC0002692 in MIBiG. Our research findings suggest that the products encoded by these two BGCs are quite similar.

The diversity and novelty of secondary metabolites produced by two representative strains, *A. albata* JCM 9917 and *K. phytohabitans* KLBMP1111were extensively investigated using HiTES experiments. The results showed that about 82% (annotation score less than 3, 0.4, or 0.5 for the Dereplicator+, FBMN, and SIRIUS analysis) of the features could not be successfully annotated, indicating their great potential to be novel natural products. Besides, the annotating results of some features with different tools were inconsistent, further emphasizing the novelty of these features. Through mass spectrometry-guided strategies, we successfully isolated and identified two siderophores, one of which is novel (N-deoxy arthrobactin A), while the remaining compounds were primarily derivatives of deoxygenation or demethylation. However, due to the low yield, we were unable to isolate the potential novel compounds identified by mass spectrometry analysis. In future studies, we will optimize the fermentation conditions to isolate these promising molecules.

In conclusion, the present study systematically compared the genus-specificity of *Allokutzneria* and *Kibdelosporangium* in secondary metabolism, highlighting their great variations in the distribution of the potential novel GCFs and the distinct metabolic profiles of two representative strains of these two genera. Two *Allokutzneria*-specific natural products, Arthrobactin A and N-deoxy arthrobactin A, were isolated and characterized for the first time from this rare genus. The present study offers valuable insights for the targeted discovery of genus-specific natural products from *Allokutzneria* and *Kibdelosporangium*.

CRediT authorship contribution statement

Man-Jing Ma: performed the experiment and prepared the original draft. **Wen-Chao Yu:** prepared the original draft and analyzed the data. **Huai-Ying Sun:** performed the experiment. **Bing-Cheng Dong:** performed the experiment. **Gang-Ao Hu:** provided technical help. **Zhen-Yi Zhou:** provided technical help. **Yi Hua:** provided helpful discussions. **Buddha Bahadur Basnet:** analyzed the NMR data. **Yan-Lei Yu:** provided helpful discussions. **Hong Wang:** conceived and designed the study. **Bin Wei:** conceived and designed the study, and revised the original draft. All authors have read and agreed to the published version of the manuscript.

Declaration of competing interest

The authors declare that they have no known competing financial interests or personal relationships that could have appeared to influence the work reported in this paper.

Acknowledgments

This work was financially supported by the Fundamental Research Funds for the Provincial Universities of Zhejiang (No. RF-A2022013), the program of the National Natural Science Foundation of China (No.

42276137), the National Key Research and Development Programs (Nos. 2022YFC2804104, and 2022YFC2804700).

Appendix A. Supplementary data

Supplementary data to this article can be found online at https://doi.org/10.1016/j.synbio.2024.03.015.

References

[1] Chater KF. *Streptomyces* Inside-out: a new perspective on the bacteria that provide us with antibiotics. Philos Trans R Soc Lond B Biol Sci 2006;361:761–8. https://doi.org/10.1098/rstb.2005.1758.

[2] Hindra, Pak P, Elliot MA. Regulation of a novel gene cluster involved in secondary metabolite production in *Streptomyces coelicolor*. J Bacteriol 2010;192:4973–82. https://doi.org/10.1128/jb.00681-10.

[3] Tiwari K, Gupta RK. Rare Actinomycetes: a potential storehouse for novel antibiotics. Crit Rev Biotechnol 2012;32:108–32. https://doi.org/10.3109/07388551.2011.562482.

[4] Bérdy J. Bioactive microbial metabolites. J Antibiot (Tokyo) 2005;58:1–26. https://doi.org/10.1038/ja.2005.1.

[5] Shearer MC, Colman PM, Ferrin RM, Nisbet LJ, Nash CH. New genus of the actinomycetales: *Kibdelosporangium aridum* gen. nov., sp. nov. Int J Syst Bacteriol 1986;36:47–54. https://doi.org/10.1099/00207713-36-1-47.

[6] Shearer MC, Actor P, Bowie BA, Grappel SF, Nash CH, Newman DJ, Oh YK, Pan CH, Nisbet LJ. Aridicins, novel glycopeptide antibiotics. I. Taxonomy, production and biological activity. J Antibiot 1985;38:555–60. https://doi.org/10.7164/antibiotics.38.555.

[7] Folena-Wasserman G, Poehland BL, Yeung EW, Staiger D, Killmer LB, Snader K, Dingerdissen JJ, Jeffs PW. Kibdelins (AAD-609), novel glycopeptide antibiotics. II. Isolation, purification and structure. J Antibiot (Tokyo) 1986;39:1395–406. https://doi.org/10.7164/antibiotics.39.1395.

[8] Labeda DP, Kroppenstedt RM. Proposal for the new genus *Allokutzneria* gen. nov. within the suborder *Pseudonocardineae* and transfer of *Kibdelosporangium albatum* Tomita et al. 1993 as *Allokutzneria albata* comb. Nov. Int J Syst Evol Micr 2008;58:1472–5. https://doi.org/10.1099/ijs.0.65474-0.

[9] Duangmal K, Poomthongdee N, Pathom-aree W, Takè A, Thamchaipenet A, Matsumoto A, Takahashi Y. *Allokutzneria oryzae* sp. nov., isolated from rhizospheric soil of Oryza sativa L. Int J Syst Evol Micr 2014;64:3559–64. https://doi.org/10.1099/ijs.0.065169-0.

[10] Izumikawa M, Takagi M, Shin-ya KJBIR-78. JBIR-95: phenylacetylated peptides isolated from *Kibdelosporangium* sp. AK-AA56. J Nat Prod 2012;75:280–4. https://doi.org/10.1021/np2008279.

[11] Rinkel J, Lauterbach L, Rabe P, Dickschat JS. Two diterpene synthases for spiroalbatene and cembrene A from *Allokutzneria Albata*. Angew Chem Int Ed Engl 2018;57:3238–41. https://doi.org/10.1002/anie.201800385.

[12] Hoshino S, Okada M, Awakawa T, Asamizu S, Onaka H, Abe I. Mycolic acid containing bacterium stimulates tandem cyclization of polyene macrolactam in a lake sediment derived rare actinomycete. Org Lett 2017;19:4992–5. https://doi.org/10.1002/anie.201800385.

[13] Wei B, Du A-Q, Zhou Z-Y, Lai C, Yu W-C, Yu J-B, Yu Y-L, Chen J-W, Zhang H-W, Xu X-W, Wang H. An atlas of bacterial secondary metabolite biosynthesis gene clusters. Environ Microbiol 2021;23:6981–92. https://doi.org/10.1111/1462-2920.15761.

[14] Wei B, Du A-Q, Ying T-T, Hu G-A, Zhou Z-Y, Yu W-C, He J, Yu Y-L, Wang H, Xu X-W. Secondary metabolic potential of *Kutzneria*. J Nat Prod 2023;86:1120–7. https://doi.org/10.1021/acs.jnatprod.3c00007.

[15] Parks DH, Imelfort M, Skennerton CT, Hugenholtz P, Tyson GW. CheckM: assessing the quality of microbial genomes recovered from isolates, single Cells, and metagenomes. Genome Res 2015;25:1043–55. https://doi.org/10.1111/1462-2920.15761.

[16] Blin K, Shaw S, Augustijn HE, Reitz ZL, Biermann F, Alanjary M, Fetter A, Terlouw BR, Metcalf WW, Helfrich EJN, van Wezel GP, Medema MH, Weber T. antiSMASH 7.0: new and improved predictions for detection, regulation, chemical structures and visualisation. Nucleic Acids Res 2023;51:W46–50. https://doi.org/10.1093/nar/gkad344.

[17] Wei B, Hu G-A, Zhou Z-Y, Yu W-C, Du A-Q, Yang C-L, Yu Y-L, Chen J-W, Zhang H-W, Wu Q, Xuan Q, Xu X-W, Wang H. Global analysis of the biosynthetic chemical space of marine prokaryotes. Microbiome 2023;11:144. https://doi.org/10.1186/s40168-023-01573-3.

[18] Kautsar SA, van der Hooft JJJ, de Ridder D, Medema MH. BiG-SLiCE: a highly scalable tool maps the diversity of 1.2 million biosynthetic gene clusters. GigaScience 2021;10:giaa154. https://doi.org/10.1093/gigascience/giaa154.

[19] Pluskal T, Castillo S, Villar-Briones A, Oresic M. MZmine 2: modular framework for processing, visualizing, and analyzing mass spectrometry-based molecular profile data. BMC Bioinf 2010;11:395. https://doi.org/10.1186/1471-2105-11-395.

[20] Nothias L-F, Petras D, Schmid R, Dührkop K, Rainer J, Sarvepalli A, Protsyuk I, Ernst M, Tsugawa H, Fleischauer M, et al. Feature-based molecular networking in the GNPS analysis environment. Nat Methods 2020;17:905–8. https://doi.org/10.1038/s41592-020-0933-6.

[21] Mohimani H, Gurevich A, Shlemov A, Mikheenko A, Korobeynikov A, Cao L, Shcherbin E, Nothias L-F, Dorrestein PC, Pevzner PA. Dereplication of microbial metabolites through database search of mass spectra. Nat Commun 2018;9:4035. https://doi.org/10.1038/s41467-018-06082-8.

[22] Dührkop K, Fleischauer M, Ludwig M, Aksenov AA, Melnik AV, Meusel M, Dorrestein PC, Rousu J, Böcker S. Sirius 4: a rapid tool for turning tandem mass spectra into metabolite structure information. Nat Methods 2019;16:299–302. https://doi.org/10.1038/s41592-019-0344-8.

[23] Bittremieux W. Spectrum_utils : a python package for mass spectrometry data processing and visualization. Anal Chem 2020;92:659–61. https://doi.org/10.1021/acs.analchem.9b04884.

[24] Chen J, Guo Y, Wu Q, Wang W, Pan J, Chen M, Jiang H, Yin Q, Zhang G, Wei B, Zhang H, Wang H. Discovery of new siderophores from a marine *Streptomycetes* sp. via combined metabolomics and analysis of iron-chelating activity. J Agric Food Chem 2023;71:6584–93. https://doi.org/10.1021/acs.jafc.3c00234.

[25] Linke WD, Crueger A, Diekmann H. Metabolic products of microorganisms: 106. The structure of Terregens factor. Arch Mikrobiol 1972;85:44–50. https://doi.org/10.1007/BF00425143.

[26] Acquah KS, Beukes DR, Warner DF, Meyers PR, Sunassee SN, Maglangit F, Deng H, Jaspars M, Gammon DW. Novel south african rare actinomycete *Kribbella speibonae* strain SK5: a prolific producer of hydroxamate siderophores including new dehydroxylated congeners. Molecules 2020;25:2979. https://doi.org/10.3390/molecules25132979.

[27] Van Santen JA, Poynton EF, Iskakova D, McMann E, Alsup TA, Clark TN, Fergusson CH, Fewer DP, Hughes AH, McCadden CA, Parra J, Soldatou S, Rudolf JD, Janssen EM-L, Duncan KR, Linington RG. The natural products atlas 2.0: a database of microbially-derived ntural products. Nucleic Acids Res 2022;50:D1317–23. https://doi.org/10.1093/nar/gkab941.

[28] Luo Y, Enghiad B, Zhao H. New tools for reconstruction and heterologous expression of natural product biosynthetic gene clusters. Nat Prod Rep 2016;33:174–82. https://doi.org/10.1039/c5np00085h.

[29] Wang Z, Koirala B, Hernandez Y, Zimmerman M, Park S, Perlin DS, Brady SF. A naturally inspired antibiotic to target multidrug-resistant pathogens. Nature 2022;601:606–11. https://doi.org/10.1038/s41586-021-04264-x.

[30] Stephenson RC, Clarke S. Succinimide Formation from Aspartyl and Asparaginyl peptides as a model for the spontaneous degradation of proteins. J Biol Chem 1989;264:6164–70. https://doi.org/10.1016/S0021-9258(18)83327-0.

[31] Xu D, Han L, Li C, Cao Q, Zhu D, Barrett NH, Harmody D, Chen J, Zhu H, McCarthy PJ, Sun X, Wang G. Bioprospecting deep-sea actinobacteria for novel anti-infective natural products. Front Microbiol 2018;9:787. https://doi.org/10.3389/fmicb.2018.00787.

[32] Kawai K, Wang G, Okamoto S, Ochi K. The rare earth, scandium, causes antibiotic overproduction in streptomyces spp. FEMS Microbiol Lett 2007;274:311–5. https://doi.org/10.1111/j.1574-6968.2007.00846.x.

[33] Pishchany G, Mevers E, Ndousse-Fetter S, Horvath DJ, Paludo CR, Silva-Junior EA, Koren S, Skaar EP, Clardy J, Kolter R. Amycomicin is a potent and specific antibiotic discovered with a targeted interaction screen. Proc Natl Acad Sci U S A 2018;115:10124–9. https://doi.org/10.1073/pnas.1807613115.

[34] Zheng J, Li Y, Liu N, Zhang J, Liu S, Tan H. Multi-omics data reveal the effect of sodium butyrate on gene expression and protein modification in streptomyces. Genom Proteom Bioinform 2022;S1672–0229(22). https://doi.org/10.1016/j.gpb.2022.09.002. 00115-2.

[35] Seyedsayamdost MR. High-throughput platform for the discovery of elicitors of silent bacterial gene clusters. Proc Natl Acad Sci U S A 2014;111:7266–71. https://doi.org/10.1073/pnas.1400019111.

[36] Mohammadipanah F, Kermani F, Salimi F. Awakening the secondary metabolite pathways of promicromonospora kermanensis using physicochemical and biological elicitors. Appl Biochem Biotechnol 2020;192:1224–37. https://doi.org/10.1007/s12010-020-03361-3.